

Carbon Monoxide Inhalation Protects Rat Intestinal Grafts from Ischemia/Reperfusion Injury

Atsunori Nakao,^{*†} Kei Kimizuka,^{*†}
Donna B. Stolz,[‡] Joao Seda Neto,^{*†}
Takashi Kaizu,^{*†} Augustine M. K. Choi,[§]
Takashi Uchiyama,[¶] Brian S. Zuckerbraun,[†]
Michael A. Nalesnik,^{**||} Leo E. Otterbein,[§] and
Noriko Murase^{*†}

From the Thomas E. Starzl Transplantation Institute,^{*} the Center for Biologic Imaging,[‡] and the Departments of Surgery,[†] Pulmonary Allergy and Critical Care Medicine,[§] Anesthesiology and Critical Care Medicine,[¶] and Pathology,^{||} University of Pittsburgh Medical Center, Pittsburgh, Pennsylvania

Carbon monoxide (CO), a byproduct of heme catalysis by heme oxygenases, has been shown to exert anti-inflammatory effects. This study examines the cytoprotective efficacy of inhaled CO during intestinal cold ischemia/reperfusion injury associated with small intestinal transplantation. Orthotopic syngenic intestinal transplantation was performed in Lewis rats after 6 hours of cold preservation in University of Wisconsin solution. Three groups were examined: normal untreated controls, control intestinal transplant recipients kept in room air, and recipients exposed to CO (250 ppm) for 1 hour before and 24 hours after surgery. In air grafts, mRNA levels for interleukin-6, cyclooxygenase-2, intracellular adhesion molecule (ICAM-1), and inducible nitric oxide synthase rapidly increased after intestinal transplant. Histopathological analysis revealed severe mucosal erosion, villous congestion, and inflammatory infiltrates. CO effectively blocked an early up-regulation of these mediators, showed less severe histopathological changes, and resulted in significantly improved animal survival of 92% from 58% in air-treated controls. CO also significantly reduced mRNA for proapoptotic Bax, while it up-regulated anti-apoptotic Bcl-2. These changes in CO-treated grafts correlated with well-preserved CD31⁺ vascular endothelial cells, less frequent apoptosis/necrosis in intestinal epithelial and capillary endothelial cells, and improved graft tissue blood circulation. Protective effects of CO in this study were mediated via soluble guanylyl cyclase, because 1H-(1,2,4)oxadiazole (4,3- α) quinoxaline-1-one (soluble guanylyl cyclase inhibitor) completely reversed the beneficial effect conferred by CO. Perioperative CO inhalation at a low concentration resulted in protection against ischemia/reperfusion injury to intestinal grafts with pro-

longed cold preservation. (Am J Pathol 2003, 163:1587-1598)

Recent developments in the use of potent immunosuppressive drugs, technical innovations in surgery, and improvements in postoperative care have significantly improved outcomes of small intestinal transplantation (SITx), and the procedure has become the critical therapeutic modality for patients with intestinal failure.¹ However, intestinal tissue is known to be exceptionally susceptible to ischemia/reperfusion (I/R) injury and intestinal grafts frequently suffer preservation injuries, resulting in prolonged intestinal dysfunction, loss of intestinal barrier function, bacterial translocation, and posttransplant sepsis. Therefore, advances in this field will significantly improve posttransplant patient care and subsequent long-term outcome of SITx.

Although the exact mechanisms of intestinal I/R injury remain undefined, multiple factors are shown to be involved in the process. The lack of oxygen during preservation is known to initiate ATP depletion, followed by an alteration of intracellular calcium and sodium concentrations and activation of cytotoxic enzymes (eg, proteases, phospholipases).^{2,3} In addition, reperfusion of grafts generates reactive oxygen species and further promotes cell damage.⁴ As a result, death or loss of the integrity of vascular endothelial cells, consequent disruption of microcirculation, generation and release of potent inflammatory mediators (cytokines, adhesion molecules, platelet activating factors), and neutrophil infiltration are known to be characteristic features associated with I/R injuries.^{5,6}

Carbon monoxide (CO), a gaseous molecule, has been well described to be toxic and lethal to living organisms when exposed to high concentrations. However, recent evidence suggests that CO acts as a regulatory molecule in cellular and biological processes. Mammalian cells have the ability to endogenously generate CO primarily via the catalysis of heme by heme oxygenases

Supported by the National Institutes of Health (grants DK54232, CA76541, HL60234, AI42365, HL553300), the American Heart Association (grant 160332U0), and the Atorvastatin Pfizer Research Award.

LEO and NM contributed equally to this study.

Accepted for publication June 27, 2003.

Address reprint requests to Noriko Murase, M.D., Thomas E. Starzl Transplantation Institute, Department of Surgery, E1555 Biomedical Science Tower, University of Pittsburgh, Pittsburgh, PA 15213. E-mail: murase+@pitt.edu.

(HO-1, -2, -3) and, to a much lesser degree, via lipid peroxidation.⁷ HO-1, the inducible isoform, has been classified as a stress-inducible protein. It is up-regulated in response to oxidative stress and proinflammatory stimuli in the liver, heart, and kidney, and has been shown to exert potent cytoprotective and anti-apoptotic properties.⁸⁻¹⁵ CO, a byproduct of HO-1, has been demonstrated to mediate cytoprotective and anti-inflammatory effects,¹⁶⁻²¹ similar to those seen with HO-1.

Although much is known regarding the toxicity and lethality of environmental concentrations of CO, little if any progress has been made in our understanding as to how CO mediates its beneficial biological and physiological functions when used in low concentrations. Accordingly, based on the hypothesis that a low concentration of CO would provide protection against I/R injury associated with intestinal transplantation, this study examined the efficacy of CO in the rat intestinal I/R injury model with prolonged cold preservation and transplantation.

Materials and Methods

Animals

Inbred male Lewis (LEW, RT¹) rats weighing 200 to 250 g were purchased from Harlan Sprague Dawley, Inc. (Indianapolis, IN), and maintained in laminar flow cages in a specific pathogen-free animal facility at the University of Pittsburgh. Animals were fed a standard diet and provided water *ad libitum*. All procedures in this experiment were performed according to the guidelines of the Council on Animal Care at the University of Pittsburgh and the National Research Council's Guide for the Humane Care and Use of Laboratory Animals.

SITx

Orthotopic SITx with caval drainage was performed using a previously described technique.²² The entire donor small intestine from the ligament of Treitz to the ileocecal valve was isolated, perfused with 10 ml of cold University of Wisconsin solution (Viaspan; Du Pont, Wilmington, DE), and placed in University of Wisconsin solution at 4°C for 6 hours. End-to-side anastomoses between the graft aorta and the recipient infrarenal aorta, and between the graft portal vein and recipient vena cava were performed with 10-0 Novafil suture. The entire recipient intestine was removed and the enteric continuity was restored by proximal and distal end-to-end intestinal anastomoses. The entire recipient surgery usually took ~60 minutes. All recipient animals in this study were given cefamandole nafate (20 mg once a day, intramuscular injection) for 3 days after transplant surgery.

CO Exposure

Animals were exposed to CO at a concentration of 250 ppm. Briefly, 1% CO in air was mixed with air (21% oxygen) in a stainless steel mixing cylinder and then directed into a 3.70 ft³ glass exposure chamber at a flow

rate of 12 L/minute. A CO analyzer (Interscan, Chatsworth, CA) was used to continuously measure CO levels in the chamber, to maintain CO concentration at 250 ppm at all times. Animals were maintained in a CO chamber for the duration of CO exposure with regular diet and water *ad libitum*.

Experimental Groups

LEW to LEW syngenic SITx with 6 hours University of Wisconsin solution cold preservation was performed without immunosuppression. Three groups of animals were examined: group 1 consisted of unoperated normal LEW, group 2 recipients received intestinal grafts and were maintained in room air, and group 3 recipients of SITx were placed in the CO chamber for 1 hour before and for 24 hours immediately after transplant surgery. In each group, recipient animals were sacrificed at 1, 3, 6, 12, 24, and 48 hours after SITx for blood and graft intestine samples ($n = 4$ to 6 in each group at each time point). A small number (30%) of animals in group 2 was kept in the chamber without CO (room air) and sacrificed 1 to 48 hours after SITx to evaluate the influence of animal housing and after SITx recovery environment. Because animal housing environment did not cause any difference in obtained results, the air-control group in this study included recipients that were kept inside and outside of the chamber. To avoid any divergence caused by patchy changes of intestinal I/R injury, whole intestinal graft was divided into nine equal-length portions and processed as the following: first and fourth segments were used for mRNA isolation, and second and fifth segments were used for protein isolation. All remaining segments were processed for routine immunohistopathology. Peyer's patches were excluded from graft samples for mRNA and protein extraction.

Separate groups of animals were followed for 14 days after SITx to determine the efficacy of CO treatment on intestinal graft/animal survival. Because animal survival entirely depended on the function of transplanted intestinal grafts, animal survival was considered to be identical to graft survival in this model. Additional supplementary groups of animals were prepared to test the role of soluble guanylyl cyclase (sGC) and cyclic 3',5'-guanosine monophosphate (cGMP) system. A selective inhibitor of sGC, 1H-(1,2,4)oxadiazole (4,3- α) quinoxaline-1-one (ODQ) (20 mg/kg; Sigma, St. Louis, MO), was dissolved in dimethyl sulfoxide and intraperitoneally injected to recipients 30 minutes before placing in a CO chamber.^{23,24} Control animals received dimethyl sulfoxide without ODQ. Animals were sacrificed at 1 hour after SITx to determine graft blood flow and mRNA levels.

Arterial Blood Gas Analyses

To determine blood CO and O₂ levels, arterial blood samples (0.2 ml) were taken at various time points after CO inhalation (250 ppm). Carboxyhemoglobin (COHb), methemoglobin (MetHb), and oxygen saturation (SaO₂)

were measured using OSM3 Hemoximeter (Radiometer Copenhagen, Copenhagen, Denmark).

Measurement of Intestinal Blood Flow

Intestinal microvascular blood flow was monitored at 1 hour after SITx by a laser Doppler flowmeter (BLF 21D; Transonic Systems, Ithaca, NY) on the serosal surface of the graft jejunum and ileum adjacent to the mesenteric border. This measurement was repeated three times each in proximal, middle, and distal portions of the intestinal grafts (nine measurements per animal) by one of the authors (TU) without knowledge of the experimental groups. Blood flows in superior mesenteric artery and marginal artery were also analyzed.

Western Blot for HO-1

Intestinal cytosolic proteins (200 μ g) were separated by electrophoresis on 12.5% acrylamide sodium dodecyl sulfate gels and transferred to nitrocellulose membranes (Sleicher & Schuell, Keene, NH). After blocking with 5% nonfat dry milk, membranes were incubated with primary rabbit polyclonal anti-HO-1 antibody (SPA-896, 1:1000; Stressgen, Victoria, Canada) for 1 hour, then with secondary goat anti-rabbit antibody (1:2000; Pierce Chemical, Rockford, IL) for 1 hour. Membranes were developed with the SuperSignal detection systems (Pierce Chemical) and exposed to film.

Total RNA Extraction and RNase Protection Assay

Total RNA was extracted from the intestinal graft using the Trizol reagent (Life Technologies, Inc. Grand Island, NY) according to the manufacturer's instructions. RNA content was measured using 260/280 UV spectrophotometry.

An RNase protection assay was performed to determine the involvement of apoptosis-associated molecules with the Riboquant kit (Pharmingen, La Jolla, CA) according to the manufacturer's protocol. Briefly, radiolabeled anti-sense RNA multiple probes were synthesized using an *in vitro* transcription kit and rat multiprobe template set rAPO-1 (Pharmingen). 32 P-labeled probes (8.0×10^5 cpm) and sample RNA (5 μ g) were hybridized at 56°C for 16 hours and single-stranded RNAs including anti-sense RNA probes were digested by RNase per the manufacturer's protocol (Pharmingen). The protected RNA duplexes were loaded on a 40% polyacrylamide electrophoresis gel and autoradiography was measured using a PhosphorImager system (Molecular Dynamics, Krefeld, Germany). Radioactivity of mRNA bands was quantified with NIH Image (National Institutes of Health, Bethesda, MD), normalized to GAPDH, and expressed as the ratio of apoptotic gene expression/GAPDH.

SYBR Green Real-Time Reverse Transcriptase-Polymerase Chain Reaction (PCR)

mRNA expression was quantified by SYBR Green two-step, real-time reverse transcriptase-PCR for plasminogen activator inhibitor-1 (PAI-1), intercellular adhesion molecule (ICAM-1), interleukin (IL)-6, tumor necrosis factor (TNF)- α , inducible nitric oxide synthase (iNOS), cyclooxygenase-2 (COX-2), HO-1, and GAPDH. Total RNA pellets were suspended in RNase-free water, followed by removal of potentially contaminating DNA by treatment with DNase I (Life Technologies, Rockville, MD). One μ g of total RNA from each sample was used for reverse transcription with an oligo dT (Life Technologies) and a Superscript II (Life Technologies) to generate first-strand cDNA. PCR reaction mixture was prepared using SYBR Green PCR Master Mix (PE Applied Biosystems, Foster City, CA). Each sample was analyzed in duplicate using the conditions recommended by the manufacturer. The following primers were used: IL-6 sense primer, 5'-CAAAGCCAGAGTCATTCAAGC-3', anti-sense primer, 5'-GGTCCTTAGCCACTCCTTCTGT-3'; iNOS sense primer, 5'-GGAGAGATTTTTACG ACACCC-3', anti-sense primer, 5'-CCATGCATAATTTGGACTTGCA-3'; COX-2 sense primer, 5'-CTCTGCGATGCTCTTCCGAG-3', anti-sense primer, 5'-AAGGATTTGCTGCATGGCTG-3'; ICAM-1 sense primer, 5'-CGTGCGTCCATTTACACCT-3', anti-sense primer, 5'-TTAGGGCCTCCTCCTGAGC-3'; TNF- α sense primer, 5'-GGTGATCGGTC-CCAACAAGGA-3', anti-sense primer, CACGCTGGCTCAGCCACTC-3'; PAI-1 sense primer, 5'-CCGATGGGCTCGAGTATGA-3', anti-sense primer, 5'-TTGTCTGATGAGTTCAGCATCCA-3'; HO-1 sense primer, 5'-CACAAAGACCAGAGTCCCTCACAG-3' anti-sense primer, 5'-AAATCCCCTGCCACGGT-3'; and GAPDH sense primer, 5'-ATGGCACAGTCAAGGCTGAGA-3', anti-sense primer 5'-CGCTCCTGGAAGATGGTGAT-3'. Thermal cycling conditions were 10 minutes at 95°C to activate the Ampliqaq Gold DNA polymerase, followed by 40 cycles of 95°C for 15 seconds and 60°C for 1 minute on an ABI PRISM 7000 Sequence Detection System (PE Applied Biosystems). Using the manufacturer's software, real-time PCR data were blotted as the ΔR_n fluorescence signal versus the cycle number. The cycle threshold was defined as the cycle number at which the ΔR_n crosses this threshold. The expression of each gene was normalized to GAPDH mRNA content and calculated relative to control using the comparative cycle threshold method.²⁵

Serum IL-6 and Nitrite/Nitrate

Serum IL-6 concentrations were determined using a rat enzyme-linked immunosorbent assay kit (ELISA; R&D, Cambridge, MA). The serum nitrite/nitrate levels, the stable end products of NO metabolism, were measured using a commercially available test kit (Cayman, Ann Arbor, MI).

Antioxidant Power

Intestinal graft tissues were taken 1 hour after reperfusion and homogenized. Supernatant of the homogenized intestinal tissues was analyzed for total antioxidant power (Oxford Biomedical Research, Oxford, MI) according to the manufacturer's protocol. The antioxidant level in each sample was determined by the reduction of Cu^{2+} to Cu^{+} because of the combined action of all antioxidants present in the sample. Generated Cu^{+} was detected by the complex formation between Cu^{+} and bathocuproine (BC), and stable complex was detected at absorption maximum between 480 to 490 nm. The obtained absorbance values were compared to a standard curve obtained using uric acid as the reductant.

Routine Histopathology

Intestinal graft samples were fixed in 10% buffered formalin, embedded in paraffin, cut into 4- μm -thick sections, and stained with hematoxylin and eosin. Degrees of I/R injuries in the villi were blindly assessed by a pathologist (MAN), based on the extent of mucosal erosion, villous congestion, and epithelialization in at least 12 sections per animal. Mucosal erosion was defined as loss of surface mucosa exceeding approximately one-half of the villous length. Villous congestion was a low-power assessment of vascular congestion in the upper mucosal/villous region. Epithelialization was defined as the presence of a flattened mucosal epithelial region with or without associated erosion. A semiquantitative grading system was applied to the histological variables based on the approximate percentage of the total sample involved with the individual process. Although the grading system is a reflection of the extent of the change, it generally also correlates with the severity of the change. Grade 0 showed involvement in <5% of the overall sample, grade 1, 6 to 25%; grade 2, 26 to 50%; grade 3, 51 to 75%; and grade 4, >75%.

Immunohistochemical Staining

Formalin-fixed, paraffin-embedded graft tissue was cut into 5- μm sections for activated caspase-3 stain using the avidin-biotin-peroxidase complex method after antigen retrieval. Endogenous peroxidase activity was blocked with superblock (Scy Tek Laboratories, Logan, UT). Sections were incubated with anti-cleaved caspase-3 polyclonal antibody (1:100; Cell Signaling Technology, Beverly, MA) overnight at 4°C, followed with biotinylated goat anti-rabbit IgG for 1 hour at room temperature (DAKO, Glostrup, Denmark). The immune complex was visualized with 3-amino-9-ethyl carbazole and hematoxylin counterstaining.

For CD31 immunofluorescent stain, graft tissues were frozen in OCT (Optimal Cold Temperature; Sakura Finetek, Inc., Torrance, CA) cut into 4- μm sections, and fixed with 2% paraformaldehyde. After blocking with 20% (v/v) normal goat serum, the tissue was stained with mouse anti-rat CD31 (PE-CAM, 1:100; Serotec, Raleigh,

NC) for 1 hour, then incubated for 1 hour with Alexa 488 (Molecular Probes, Eugene OR) conjugated goat anti-mouse IgG antibody. F-Actin was visualized by staining with rhodamine-phalloidin (1:250, Molecular Probes) for 30 minutes, then with Hoechst dye (bisBenzimide, 1 μg /100 ml) for 30 seconds to stain nuclear DNA. The sections were washed and coverslipped with Gelvatol, a water-soluble mounting media [23 g polyvinyl alcohol, 50 ml glycerol, 0.01% sodium azide in 100 ml of phosphate-buffered saline (PBS)], and visualized with an Olympus BX51 epifluorescence microscope and digitized with an Olympus color video camera.

Transmission Electron Microscopy

Intestines were immersion fixed in 2.5% glutaraldehyde overnight at 4°C, washed three times in PBS, then post-fixed in aqueous 1% OsO_4 , 1% $\text{K}_3\text{Fe}(\text{CN})_6$ for 1 hour. After three PBS washes, the tissue was dehydrated through a graded series of 30 to 100% ethanol, 100% propylene oxide, then infiltrated in 1:1 mixture of propylene oxide:Polybed 812 epoxy resin (Polysciences, Warrington, PA) for 1 hour. After several changes of 100% resin throughout 24 hours, tissue was embedded in molds, cured at 37°C overnight, followed by additional hardening at 65°C for 2 more days. Ultrathin (70 nm) sections were collected on 200-mesh copper grids, stained with 2% uranyl acetate in 50% methanol for 10 minutes, followed by 1% lead citrate for 7 minutes. Sections were photographed using a JEOL JEM 1210 transmission electron microscope (JEOL, Peabody, MA) at 80 kV onto electron microscope film (ESTAR thick base; Kodak, Rochester, NY). Electron micrographs were digitized on a flatbed scanner at 400 ppi (Studiostar; Agfa, Ridgefield Park, NJ). Digitized images were assembled into montages using Adobe Photoshop 6.1.

Vascular Corrosion Casting

The abdominal aorta was cannulated with 20 gauge IV catheter and clamped above the superior mesenteric artery. After blood was flushed from the intestinal vasculature using cold lactate Ringer solution, the vasculature was then perfused with Batson's no. 17 methyl methacrylate prepared according to the manufacturer's directions (Polysciences). Casting solution was allowed to polymerize for 1 hour at 4°C, intestines were removed from the animal and 2-cm sections were collected, cut open, then pinned luminal side up onto dental wax. Polymerization was allowed to continue overnight at 4°C. Tissue was then placed into several changes of 10% NaOH solution at room temperature throughout a 1-week period. When connective tissues were removed and vascular casts appeared clean, samples were washed 10 to 15 times with distilled water throughout a 2-day period. After drying at room temperature overnight, the casts were mounted onto aluminum stubs coated with copper double-stick tape, grounded with silver paint, sputter-coated with 3.5 nm of gold-palladium (108 Auto; Cressington,

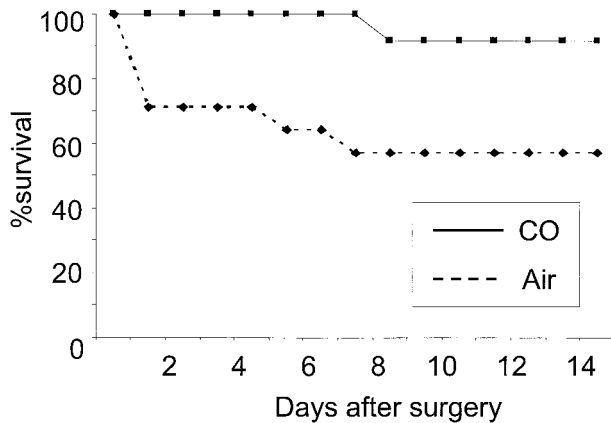


Figure 1. Effect of CO on animal survival after 6 hours of cold preservation of intestinal grafts. Fourteen-day survival of air-treated recipients (58.3%, 7 of 12) significantly ($P < 0.05$) improved with CO to 91.7% (11 of 12).

Cranberry, PA) and viewed at 5 kV on a JEOL 6330 scanning electron microscope (JEOL).

Data Analysis

Results are expressed as mean \pm SD. Statistical analysis was performed using Student's *t*-test or analysis of variance where appropriate. A probability level of $P < 0.05$ was considered statistically significant.

Results

Blood Gas and COHb in CO-Treated Animals

When animals were kept in the CO chamber, they were observed every 1 to 3 hours. Water and food consumption and body weight gain during and after CO inhalation were not different from those kept in room air. One-hour CO inhalation resulted in the elevation of COHb to $20.5 \pm 6.0\%$ from $1.6 \pm 0.7\%$ in the room air. When animals were removed from the CO chamber to room air for transplant surgery, COHb levels decreased to $13.7 \pm 0.1\%$ by the end of surgery. Thus, COHb levels in recipients were between 13% and 22% throughout the experiment. MetHb levels were $<1\%$ at all time points. Blood oxygen saturation was 100.4 ± 2.2 in room air and 101.7 ± 3.9 at the end of 24 hours of CO inhalation.

Animal Survival and Clinical Course

Six hours of cold preservation in University of Wisconsin solution of the intestinal graft induced intestinal dysfunction in untreated recipients; 3 of 12 control animals died within 24 hours and an additional 2 animals died 5 and 7 days after SITx because of bowel obstruction secondarily to intestinal I/R injury. In contrast, all CO-treated animals recovered smoothly from SITx, and only 1 of 12 CO-treated animals died of bowel obstruction on day 8. Overall animal survival for 14 days of follow-up was 58.3% (7 of 12) in air control and 91.7% (11 of 12) in CO-treated group ($P < 0.05$) (Figure 1).

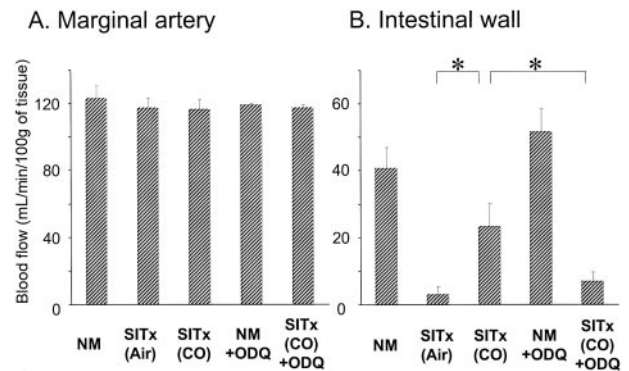


Figure 2. Laser Doppler flowmeter measurements of graft blood flows of marginal artery (A) and intestinal wall (B). A: Blood flows of intestinal marginal artery were similar in all groups. B: CO inhalation significantly increased intestinal graft blood flow to 23.2 ± 7.0 ml/minute/100 g compared to <4 ml/minute/100 g in air-treated grafts. Intestinal microcirculation of normal and ODQ-treated unoperated animals was ~ 40 ml/minute/100 g. ODQ (20 mg/kg) administration to recipient 30 minutes before CO treatment completely abrogated CO effect and intestinal blood flow was 6 ml/minute/100 g. $n = 3$ to 4 for each group. *, $P < 0.05$. NM, normal.

Blood Flow in the Graft Intestine

CO has been known to play an important role in regulating vasomotor tone by promoting vasorelaxation through sGC activation.^{26,27} Blood flows of the intestinal major vessels (superior mesenteric artery and marginal artery) were not different in normal unoperated and transplanted intestine, regardless of CO, and maintained between 116 and 126 ml/minute/100 g (Figure 2). Microvascular blood flow of normal intestine was 40.7 ± 6.3 ml/minute/100 g. In air-treated control graft intestine, blood flow was barely detected (<4 ml/minute/100 g), whereas CO-treated intestinal grafts showed a significantly ($P < 0.05$) increased flow rate (23.2 ± 7.0 ml/minute/100 g).

PAI-1 mRNA Expression

PAI-1 is the main inhibitor of tissue type (t-PA) and urokinase type (u-PA) plasminogen activators and reduces fibrinolysis,²⁸ and has been shown to be inhibited by CO in mouse lung injury model.²⁷ The involvement of PAI-1 in this study was analyzed by PCR. mRNA for PAI-1 was up-regulated during intestinal I/R injury with a peak at 6 hours. CO treatment did not influence PAI-1 mRNA levels (Figure 3A).

Inflammatory Mediators

mRNA levels for inflammatory cytokines (IL-6, TNF- α), stress-induced molecules (iNOS, COX-2), and adhesion molecule (ICAM-1) promptly increased in air-treated graft intestine, peaking at 1 to 6 hours after reperfusion. Exposure to CO inhibited mRNA up-regulation of these mediators. The increase in TNF- α mRNA in the cold-preserved control intestinal graft was modest, and CO inhalation did not affect TNF- α mRNA expression (Figure 3; B to F).

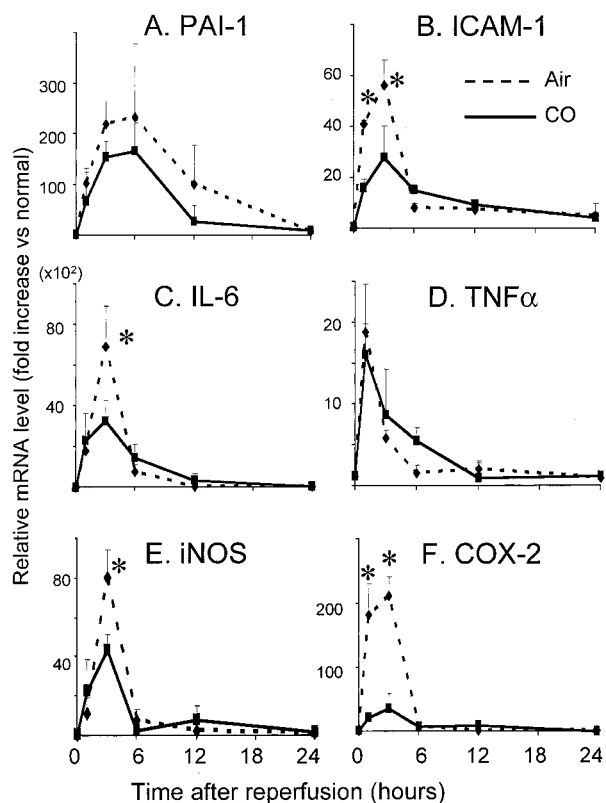


Figure 3. mRNA expression in intestinal grafts. **A:** mRNA for PAI-1 was up-regulated during I/R injury in air-treated controls with a peak at 6 hours. CO treatment tended toward a reduction in the expression of PAI-1 but statistical significance was not achieved. Cytokine and inflammatory mediator mRNA expressions of ICAM-1 (**B**), IL-6 (**C**), TNF- α (**D**), iNOS (**E**), and COX-2 (**F**) were evaluated in CO versus air-treated grafts. These mediators, except for TNF- α , were significantly reduced with CO inhalation. Of note, COX-2 was reduced with CO to <30% of control. $n = 4$ to 6 for each group. *, $P < 0.05$.

In accordance with mRNA levels, serum IL-6 was rapidly elevated in air-treated animals, peaking at 6 hours after SITx (Figure 4). CO significantly decreased peak serum IL-6 levels. In addition, intestinal I/R injury resulted in an increase in serum nitrite/nitrate in air-treated recipients, which was suppressed in recipients treated with CO (Figure 4).

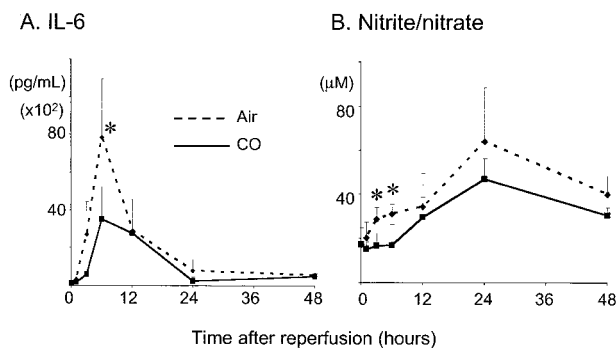


Figure 4. Analysis of serum IL-6 (**A**) and nitrate/nitrite (**B**). **A:** Serum IL-6 rapidly elevated and peaked at 6 hours in air-treated controls. Similarly to mRNA expression, CO treatment significantly decreased serum IL-6. **B:** Serum nitrate/nitrite gradually increased for 24 hours during I/R injury in air-treated animals, which was reduced by CO with statistical significance ($P < 0.05$) at 3 and 6 hours.

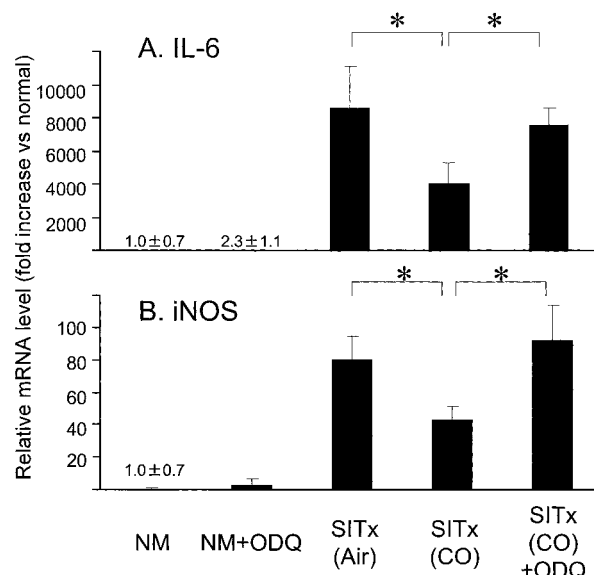


Figure 5. ODQ reverses CO-induced anti-inflammatory effects. Reduction of mRNA for IL-6 and iNOS by CO treatment was abrogated in animals treated with ODQ. ODQ administration to CO-treated animals restored IL-6 and iNOS mRNA expression comparable to air control grafts 3 hours after reperfusion. ODQ did not alter mRNA expression of these mediators in unoperated normal animals. $n = 3$ for each group. *, $P < 0.05$. NM, normal.

Effects of sGC Inhibitor

To investigate a potential mechanism involved in CO treatment, ODQ (selective inhibitor of sGC) was administered to CO-treated recipients. Although CO alone improved intestinal blood flow to >20 ml/minute/100 g in SITx recipients, ODQ administration to CO-treated recipients significantly reduced it to 6.9 ± 2.9 ml/minute/100 g. ODQ alone did not alter blood flow in unoperated normal rat intestine (see Figure 2). Furthermore, although CO treatment inhibited increases in mRNA for inflammatory mediators (see Figure 3); animals treated with ODQ in the presence of CO showed a reversal in the effects of CO on IL-6 and iNOS to the levels comparable to air-treated control grafts ($n = 3$) (Figure 5). These results suggest that cGMP may be a key mediator responsible for the effects observed with CO treatment in this model.

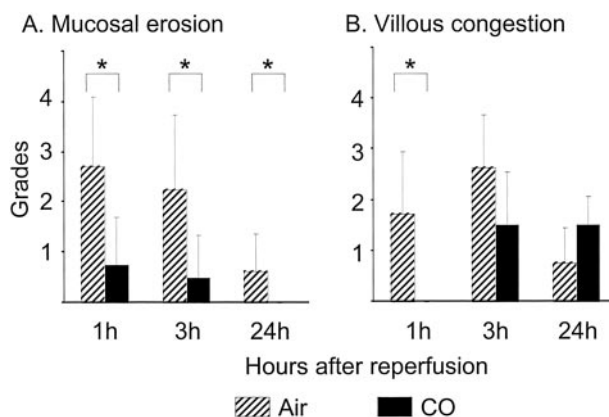


Figure 6. Severity of mucosal injury assessed by routine histopathology. Intestinal cold I/R injury associated with intestinal epithelial cell loss and mucosal erosion (**A**), and villous congestion observed in air-treated control grafts (**B**). CO-treated grafts showed significantly less severe injury. $n = 6$ for each group. *, $P < 0.05$.

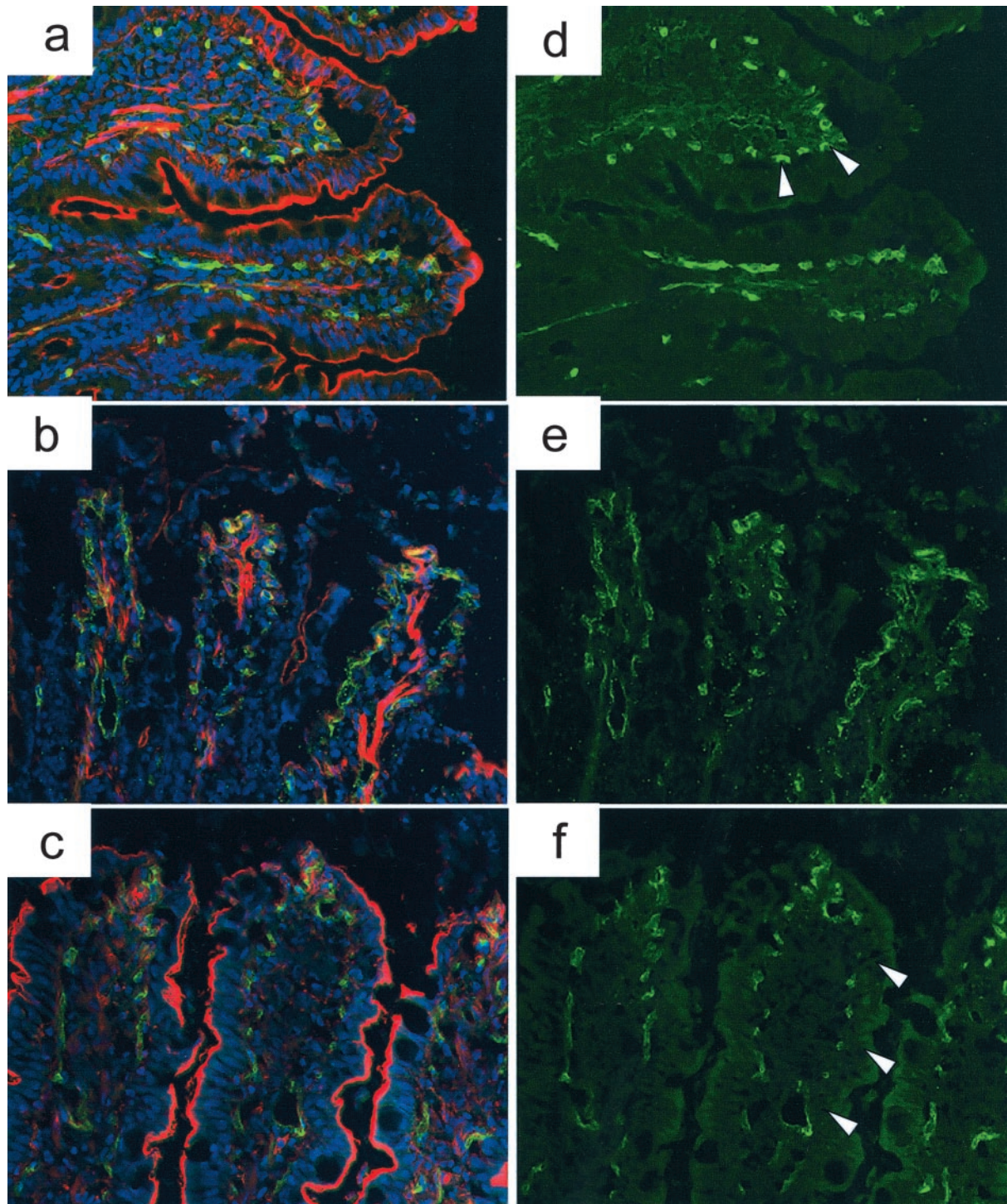


Figure 7. CD31 expression of vascular endothelial cells. **a** and **d**: Immunofluorescent stain of CD31 revealed an abundant expression of CD31 on the vascular endothelial cells in normal intestinal lamina propria. F-actin, which indicates intestinal epithelial microvilli, is also well visualized on the entire villi of normal intestine. **b** and **e**: CD31 expression was faint and interrupted in air-treated intestinal grafts after cold I/R injury, and F-actin stain was either disrupted in the upper half of the villi or weak in the remaining villi (air-treated grafts, 1 hour after reperfusion). **c** and **f**: CD31-positive vascular endothelial cells were preserved in the lamina propria of CO-treated grafts with F-actin stain revealing normal intestinal microvilli preservation (CO-treated graft, 1 hour after SITx). Green, CD31; red, F-actin; blue, nuclei. Original magnifications, $\times 400$.

Intestinal Graft Histopathology

Shortly after reperfusion of air-treated control grafts, there was a massive loss of intestinal epithelial cells, resulting in mucosal erosion and moderate villous congestion in

>50% of the villi by 3 hours. CO treatment significantly reduced these histopathological changes of I/R injury and showed nearly intact intestinal histopathology (Figure 6).

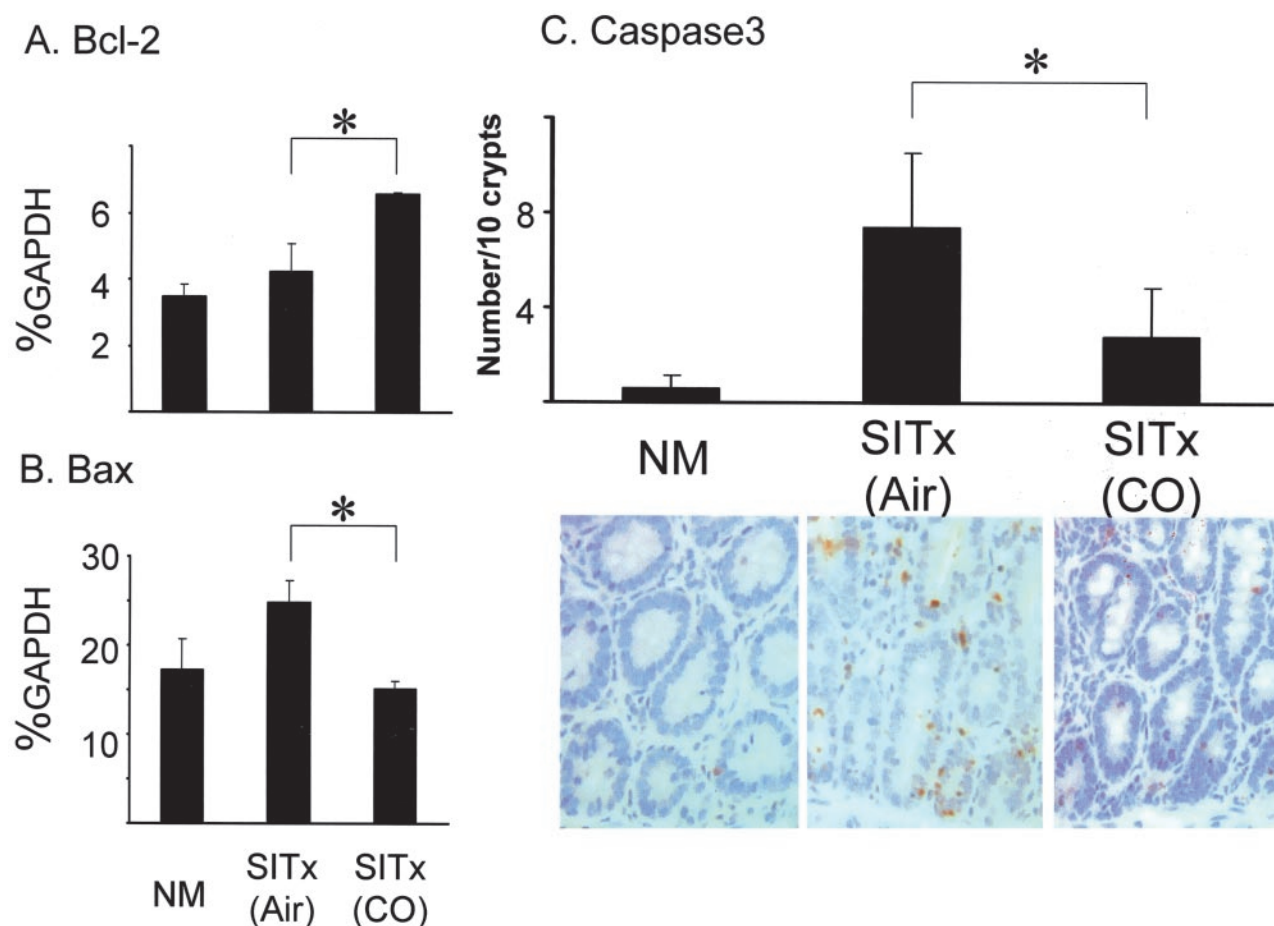


Figure 8. Apoptosis-related molecules in intestinal grafts. **A:** There is a twofold increase of anti-apoptotic Bcl-2 in CO-treated grafts compared to air-treated controls at 1 hour after reperfusion. **B:** Bax, a proapoptotic gene, was significantly up-regulated 1 hour in air control ($P < 0.05$), which was not observed in CO-treated grafts. **C:** Numbers of activated caspase 3-positive cells increased in crypt epithelial cells of air control. CO significantly ($P < 0.05$) reduced caspase 3-stained apoptotic crypt epithelial cells. NM, normal intestine.

Endothelial Cell Injury and CD31 Stain

Vascular endothelial cells have been known to be a main target of I/R injury, leading to the disruption of microcirculation in the transplanted organs. Because CO in this study is shown to improve intestinal graft blood flow, morphological changes of vascular endothelial cells were further analyzed by the pan-endothelial cell marker, CD31. CD31 was abundantly expressed on the endothelial cells of the capillaries in normal intestinal lamina propria (Figure 7). In air-treated grafts, CD31 expression was considerably reduced, irregular, and interrupted indicating severe vascular endothelial cell injury. CO-treated grafts demonstrated relatively normal CD31 expression on lamina propria capillaries, suggesting the preservation of vascular endothelial cells with CO during I/R stress.

F-actin stain, which indicates intestinal epithelial microvilli, was either disrupted in the upper half of the villi or faint in the remaining regions of air-treated control grafts. In contrast, most of the villi in CO-treated grafts showed relatively clear F-actin staining and preservation of epithelial microvilli, except for the utmost apex of the villi

where some of the intestinal epithelial cells were lost (Figure 7).

Apoptosis-Associated Molecules

mRNA for proapoptotic gene Bax increased in air-treated intestinal grafts at 1 hour. CO blocked early Bax up-regulation (Figure 8B). Likewise, mRNA levels for anti-apoptotic Bcl-2 were significantly higher at 1 hour in CO-treated *versus* air-treated grafts (Figure 8B). There was no significant difference in Bax and Bcl-2 mRNA levels between CO- and air-treated grafts at 6 to 24 hours after reperfusion (data not shown). In addition, immunohistochemistry for activated caspase-3 was performed to evaluate apoptosis in the intestinal mucosa. Activated caspase-3-positive cells increased to 7.4 ± 3.1 per 10 crypts in air control, while 0.6 ± 0.5 cells in normal intestine. In CO-treated grafts, 2.8 ± 2.0 positive crypt epithelial cells were noted with a significant reduction compared to air-treated grafts (Figure 8).

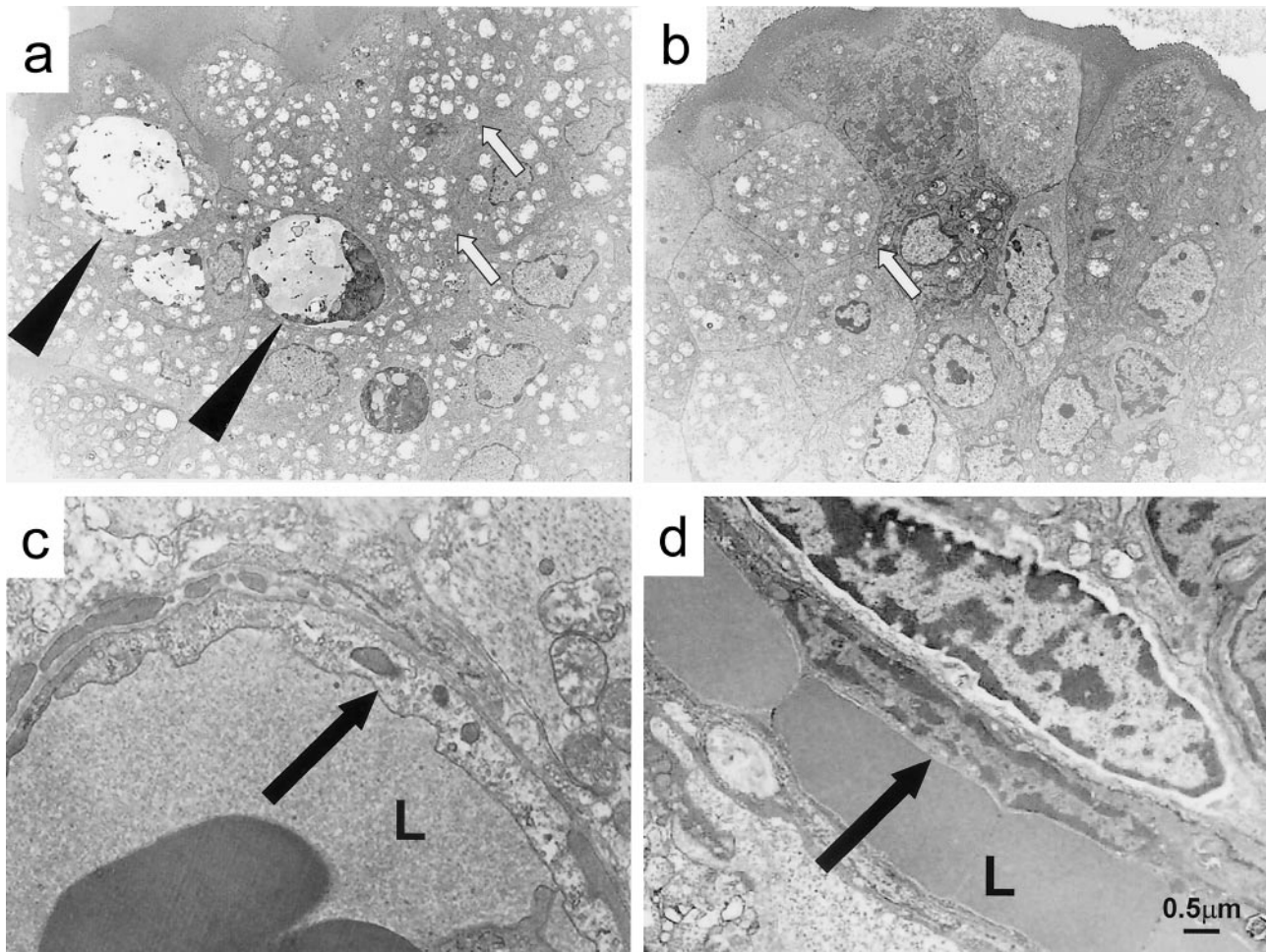


Figure 9. Transmission electron microscopy of intestinal grafts. **a:** Numerous vacuolization (**white arrows**) and apoptotic bodies (**black arrows**) are present in epithelial cells of air exposed control grafts. **b:** CO-treated grafts contain minimum apoptotic bodies and considerably less vacuolization. **c:** In the air-exposed controls, vascular endothelial cells in the lamina propria showed karyolytic nuclei with disorganized internal architecture (**arrow**). **d:** Endothelial cells in the CO-treated grafts were well maintained and demonstrated a normal intracellular architecture (**arrow**). **a–d:** 1 hour after reperfusion. L, lumen of blood vessels. Scale bar, 0.5 μm . Original magnifications: $\times 1500$ (**a, b**); $\times 5000$ (**c, d**).

Transmission Electron Microscopy

We have conducted transmission electron microscopy to further analyze the effects of CO on detailed morphological changes and integrity of vascular endothelial cells and epithelial cells of the intestine. Numerous vacuolizations were noted in intestinal epithelial cells at the bottom of the villi of untreated grafts, indicating the mitochondrial breakdown and irreversible degeneration. In correlation with Bcl-2 and Bax mRNA expression, there was a considerable increase of apoptosis in the epithelial cells of air-treated grafts. In CO-treated grafts, vacuolization was less frequent and only minimum numbers of apoptotic bodies were identified. Vascular endothelial cells in the lamina propria of the air-exposed control animals showed extensive damage as evidenced by light cytoplasmic staining and disorganization of the internal cellular architecture. However, the endothelial cells in the CO-exposed recipients were well maintained with normal features (Figure 9).

Vascular Casting

Vascular casting and scanning electron microscopy (SEM) visualized three-dimensional structure of the fine vascular arrangements or connections in the intestinal villi. Using this method, the effect of CO inhalation on graft microvascular circulation was evaluated. Utilization of this method in normal animals indicated that the afferent artery, after reaching the apex of the villus, gave rise to the capillary plexus, which collects at the base of the villus, evolving into the efferent vein as reported previously.²⁹

In air-treated grafts, there was an exudation of casting resin and pooling into the villous plexus of the lamina propria. A significant number of filling defects in the networks of capillaries were observed, indicating interruptions in vascular integrity. These findings demonstrated that afferent arteries present in the lamina propria of the graft were leaky, most likely because of endothelial injury. However, CO provided almost complete protection

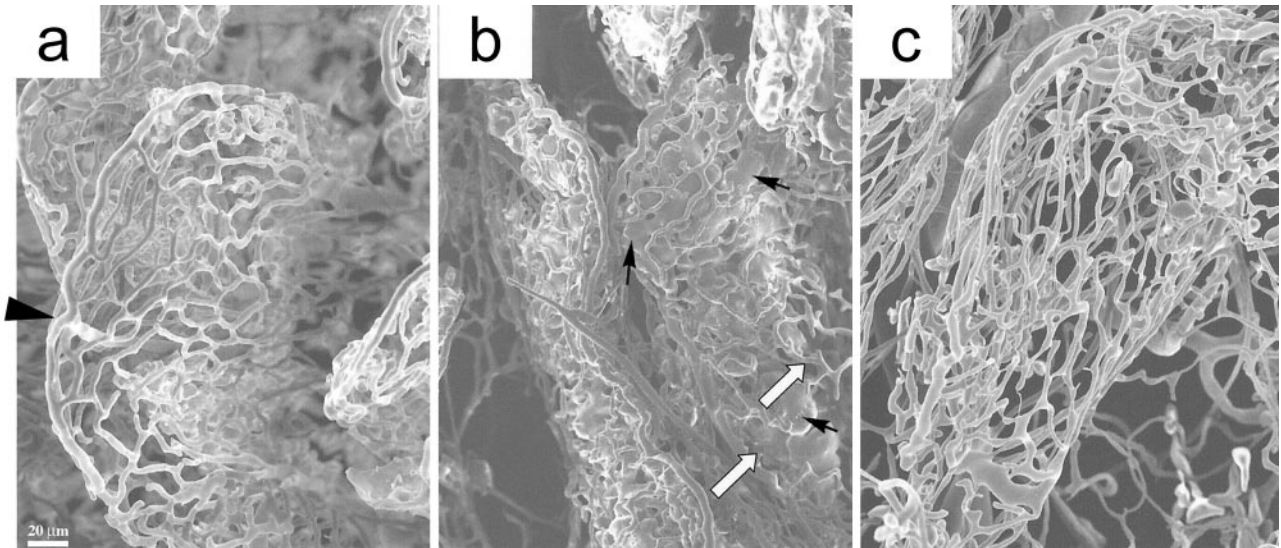


Figure 10. Scanning electron microscopy of graft vascular cast. **a:** Normal intestine showed typical hollow arrangement of vessels that comprise the villi vasculature (**arrowhead**, afferent artery reaching the apex of the villous and giving rise to the villous capillary). **b:** Severe leakage (collection of methyl methacrylate, **black arrow**) with interruption of vascular cast (**white arrow**) was evident in the internal sections of the villi (air-treated, 1 hour). **c:** Nearly normal villous vasculature was obtained without leakage (CO-treated, 1 hour). Scale bar, 20 μ m.

against such a leakage, showing clear features of vascular network similar to those observed in normal intestine (Figure 10).

HO-1 Expressions

To examine the influence of CO treatment on endogenous HO-1 induction, mRNA and protein levels of HO-1 were analyzed in intestinal tissues from air-control and CO-treated recipients. The real-time PCR for HO-1 showed an up-regulation of HO-1 mRNA expression in air-treated grafts with peaks at 3 and 6 hours after transplantation (Figure 11A). CO treatment did not significantly alter HO-1 mRNA levels.

In the Western blot, HO-1 protein was absent in the normal untreated intestine. In air-treated grafts, I/R injury

was associated with a gradual increase of HO-1 expression (Figure 11B), reaching maximum level between 6 and 24 hours after reperfusion. Intestinal grafts from CO-treated recipients showed similar levels and patterns of endogenous HO-1 protein expression. These data suggest that CO inhalation to intestinal recipient does not affect endogenous I/R-induced up-regulation of HO-1.

Total Antioxidant Power

Normal unoperated intestine had antioxidant power of $39.2 \pm 2.0 \mu\text{mol/L/mg}$ protein. Intestinal grafts from air-treated control showed decreased antioxidant power to $16.8 \pm 5.8 \mu\text{mol/L/mg}$ protein at 1 hour after reperfusion (Figure 12). Treatment with CO significantly increased the antioxidant power in the intestinal graft to $34.1 \pm 4.2 \mu\text{mol/L/mg}$ protein, indicating that there appears to be less reactive oxygen metabolites in the CO inhalation group.

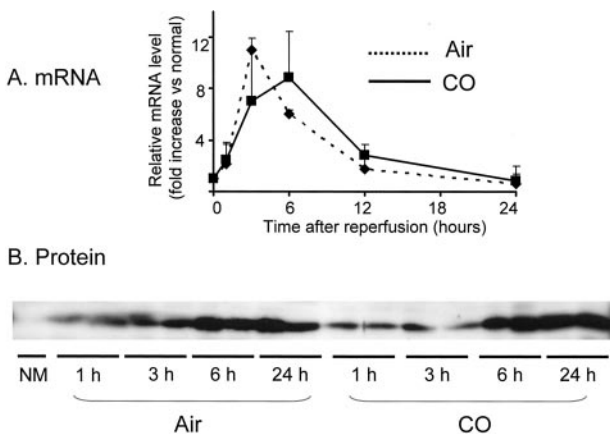


Figure 11. HO-1 mRNA (A) and protein (B) levels during intestinal I/R injury with and without CO inhalation. **A:** The real-time PCR for HO-1 showed an up-regulation of HO-1 mRNA expression in air- and CO-treated grafts with peaks at 3 and 6 hours after transplantation. **B:** Western blot showed a gradual increase of HO-1 protein expression 1 hour after reperfusion. CO treatment did not alter HO-1 protein expression. NM, normal.

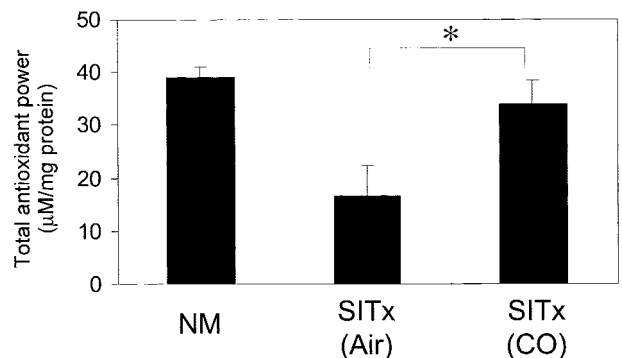


Figure 12. Antioxidant power in intestinal grafts. Intestinal I/R injury resulted in a significant reduction of antioxidant power in the air-treated control. In contrast, the CO-treated group showed preserved antioxidant power. *, $p < 0.05$.

Discussion

The heme oxygenase system has been shown to be activated in response to I/R injury and deliberated as an endogenous anti-oxidative defense mechanism, akin to several other molecules that are up-regulated during I/R injury (eg, iNOS). The beneficial role of the heme oxygenase system was substantiated when exogenous HO-1 was demonstrated to ameliorate tissue injury and induce cytoprotection.^{8–15} Furthermore, because HO-1 functions by catabolizing heme to biliverdin, iron, and CO, these byproducts of heme degradation were believed to be the effector molecules underlying the potent cytoprotection observed with the heme oxygenase system.^{16–21,30,31}

Previous reports have shown potent therapeutic benefits of CO during oxidative stress; hyperoxic lung injury; endotoxemia; and rejection of the liver, heart, and lung.^{16–21} We hypothesized that the product CO would confer protection in a model of I/R injury associated with transplantation. In this study, using an intestinal cold I/R injury model, CO was shown to be anti-inflammatory (down-regulation of proinflammatory cytokines and adhesion molecules) and anti-apoptotic (regulation of apoptosis-related molecules and reduction of vascular endothelial and intestinal epithelial apoptosis), and to preserve intestinal graft microcirculation.

Several mechanisms have been proposed to explain how CO exerts potent protective effects. The findings in this study that CO significantly improved intestinal microcirculation after cold I/R injury and that ODQ completely abrogated the beneficial effects of CO strongly suggest that the sGC/cGMP pathway is involved in the CO-mediated potent anti-I/R injury effects. CO is capable of binding and activating sGC, the enzyme that converts guanine triphosphate (GTP) to cGMP, which is an intracellular signaling molecule involved in the regulation of cellular events, such as smooth muscle relaxation, inhibition of platelet aggregation, and synaptic transmission. Several studies have shown that CO exerts potent protective effects against ischemic injury by promoting sGC/cGMP-dependent activities and thereby inhibiting platelet aggregation and smooth muscle relaxation.^{26,27,32–34} Suppression of PAI-1 induction and reduction of accrual of microvascular fibrin are also shown to occur by CO-mediated activation of this cascade.²⁷

Another mechanism by which CO mediates its protective effects against I/R injury appears to include potent anti-inflammatory actions associated with the activation of monocytes/macrophages. CO has been shown to inhibit proinflammatory cytokines (eg, TNF- α , IL-1 β) and chemokines, while simultaneously inducing anti-inflammatory cytokines (eg, IL-10) via the activation of p38 mitogen-activated protein kinase (MAPK) signaling pathway.^{18,20,35} Intestinal I/R injury resulted in a significant increase of inflammatory mediators. Although these mediators have complex roles, functional redundancy, and tissue/environment-specific activities, and the sources and definite roles of increased inflammatory mediators require further investigation, this study showed down-regulation of several proinflammatory mediators with CO

treatment. Further studies will be necessary to differentiate whether CO primarily inhibits inflammatory responses via p38 MAPK or the reduction of proinflammatory responses is secondarily induced from CO's effects on the vascular system through cGMP. Recent evidence suggests that cGMP can activate p38 MAPK,³⁶ but it remains unclear whether it is involved in the effects observed in this model.

CO-treated animals showed early up-regulation of the anti-apoptotic molecule, Bcl-2 and down-regulation of the proapoptotic signal, Bax, and reduced *in vivo* apoptosis of both vascular endothelial cells and intestinal epithelial cells. The anti-apoptotic function of CO has also been shown *in vitro* in endothelial cells, pancreatic islet cells as well as *in vivo* in a model of I/R lung injury.^{17,37,38} The anti-apoptotic function of CO is arbitrated by activation of the sGC/cGMP pathway and in other cases by the activation of p38 MAPK.^{17,39} I/R injury induces widespread endothelial cell apoptosis and promotes thrombosis directly in the intestine.⁴⁰ It is unclear whether apoptosis is the primary event associated with oxidative stress or if it is induced secondarily after the inflammatory response. Although the role of apoptosis during intestinal I/R injury needs to be studied further, inhibition of the cell death pathway may be an important strategy for the prevention of I/R injury.

It may be of interest that although CO shares many biological actions (eg, smooth muscle relaxation, inhibition of platelet aggregation) with other stress-inducible molecules, NO and COX.^{41,42} CO inhalation in this study dramatically suppressed iNOS and COX-2 expression in the transplanted grafts, while preserving endogenous HO-1 up-regulation. The results may suggest that these pathways can function independently of others. Alternatively, the inhibition of these proteins may also participate in the protective effects conferred by CO in this model. iNOS and COX-2 have been shown to be involved in the inflammatory response after oxidative stress; however, it remains to be determined whether these molecules are mediators of injury or simply markers of tissue damage.

In conclusion, inhalation of CO at a low concentration provides powerful protection of the intestine from cold I/R injury after SITx by maintaining tissue microvascular circulation, down-regulating proinflammatory responses, and inhibiting apoptosis of vascular endothelial cells and intestinal epithelial cells. CO in this study mediates the efficacy at least in part through the sGC/cGMP pathway and may potentially be useful for clinical SITx.

Acknowledgments

We thank the Thackeray Lab, Department of Bioengineering (University of Pittsburgh), for their assistance in measuring blood gas; Emeka Ifedigbo for the maintenance of the CO chamber; Mike Tabacek, Mark A. Ross, and Sean Alber for their excellent technical support; and Carla Forsythe for the preparation and organization of manuscript.

References

1. Abu-Elmagd K, Reyes J, Bond G, Mazariegos G, Wu T, Murase N, Sindhi R, Martin D, Colangelo J, Zak M, Janson D, Ezzelarab M, Dvorchik I, Parizhskaya M, Deutsch M, Demetris A, Fung J, Starzl TE: Clinical intestinal transplantation: a decade of experience at a single center. *Ann Surg* 2001, 234:404–416
2. Gores GJ, Nieminen AL, Fleishman KE, Dawson TL, Herman B, Lemasters JJ: Extracellular acidosis delays onset of cell death in ATP-depleted hepatocytes. *Am J Physiol* 1988, 255:C315–C322
3. Buderus S, Siegmund B, Spahr R, Krutzfeldt A, Piper HM: Resistance of endothelial cells to anoxia-reoxygenation in isolated guinea pig hearts. *Am J Physiol* 1989, 257:H488–H493
4. Freeman BA, Crapo JD: Biology of disease: free radicals and tissue injury. *Lab Invest* 1982, 47:412–426
5. Clavien PA, Harvey PR, Strasberg SM: Preservation and reperfusion injuries in liver allografts. An overview and synthesis of current studies. *Transplantation* 1992, 53:957–978
6. Jaeschke H: Preservation injury: mechanisms, prevention and consequences. *J Hepatol* 1996, 25:774–780
7. Poss KD, Tonegawa S: Heme oxygenase 1 is required for mammalian iron reutilization. *Proc Natl Acad Sci USA* 1997, 94:10919–10924
8. Maines MD, Mayer RD, Ewing JF, McCoubrey Jr WK: Induction of kidney heme oxygenase-1 (HSP32) mRNA and protein by ischemia/reperfusion: possible role of heme as both promoter of tissue damage and regulator of HSP32. *J Pharmacol Exp Ther* 1993, 264:457–462
9. Tacchini L, Schiaffonati L, Pappalardo C, Gatti S, Bernelli-Zazzera A: Expression of HSP 70, immediate-early response and heme oxygenase genes in ischemic-reperfused rat liver. *Lab Invest* 1993, 68:465–471
10. Amersi F, Buelow R, Kato H, Ke B, Coito AJ, Shen XD, Zhao D, Zaky J, Melinek J, Lassman CR, Kolls JK, Alam J, Ritter T, Volk HD, Farmer DG, Ghobrial RM, Busuttil RW, Kupiec-Weglinski JW: Upregulation of heme oxygenase-1 protects genetically fat Zucker rat livers from ischemia/reperfusion injury. *J Clin Invest* 1999, 104:1631–1639
11. Hangaishi M, Ishizaka N, Aizawa T, Kurihara Y, Taguchi J, Nagai R, Kimura S, Ohno M: Induction of heme oxygenase-1 can act protectively against cardiac ischemia/reperfusion in vivo. *Biochem Biophys Res Commun* 2000, 279:582–588
12. Shimizu H, Takahashi T, Suzuki T, Yamasaki A, Fujiwara T, Odaka Y, Hirakawa M, Fujita H, Akagi R: Protective effect of heme oxygenase induction in ischemic acute renal failure. *Crit Care Med* 2000, 28:809–817
13. Kato H, Amersi F, Buelow R, Melinek J, Coito AJ, Ke B, Busuttil RW, Kupiec-Weglinski JW: Heme oxygenase-1 overexpression protects rat livers from ischemia/reperfusion injury with extended cold preservation. *Am J Transplant* 2001, 1:121–128
14. Soares MP, Brouard S, Smith RN, Bach FH: Heme oxygenase-1, a protective gene that prevents the rejection of transplanted organs. *Immunol Rev* 2001, 184:275–285
15. Katori M, Anselmo DM, Busuttil RW, Kupiec-Weglinski JW: A novel strategy against ischemia and reperfusion injury: cytoprotection with heme oxygenase system. *Transpl Immunol* 2002, 9:227–233
16. Pannen BH, Kohler N, Hole B, Bauer M, Clemens MG, Geiger KK: Protective role of endogenous carbon monoxide in hepatic microcirculatory dysfunction after hemorrhagic shock in rats. *J Clin Invest* 1998, 102:1220–1228
17. Brouard S, Otterbein LE, Anrather J, Tobiasch E, Bach FH, Choi AM, Soares MP: Carbon monoxide generated by heme oxygenase 1 suppresses endothelial cell apoptosis. *J Exp Med* 2000, 192:1015–1026
18. Otterbein LE, Bach FH, Alam J, Soares M, Tao Lu H, Wysk M, Davis RJ, Flavell RA, Choi AM: Carbon monoxide has anti-inflammatory effects involving the mitogen-activated protein kinase pathway. *Nat Med* 2000, 6:422–428
19. Kyokane T, Norimizu S, Taniai H, Yamaguchi T, Takeoka S, Tsuchida E, Naito M, Nimura Y, Ishimura Y, Suematsu M: Carbon monoxide from heme catabolism protects against hepatobiliary dysfunction in endotoxin-treated rat liver. *Gastroenterology* 2001, 120:1227–1240
20. Amersi F, Shen XD, Anselmo D, Melinek J, Iyer S, Southard DJ, Katori M, Volk HD, Busuttil RW, Buelow R, Kupiec-Weglinski JW: Ex vivo exposure to carbon monoxide prevents hepatic ischemia/reperfusion injury through p38 MAP kinase pathway. *Hepatology* 2002, 35:815–823
21. Otterbein LE: Carbon monoxide: innovative anti-inflammatory properties of an age-old gas molecule. *Antioxid Redox Signal* 2002, 4:309–319
22. Murase N, Demetris AJ, Woo J, Tanabe M, Furuya T, Todo S, Starzl TE: Graft-versus-host disease after brown Norway-to-Lewis and Lewis-to-Brown Norway rat intestinal transplantation under FK506. *Transplantation* 1993, 55:1–7
23. Schrammel A, Behrends S, Schmidt K, Koesling D, Mayer B: Characterization of 1H-[1,2,4]oxadiazolo[4,3-a]quinoxalin-1-one as a heme-site inhibitor of nitric oxide-sensitive guanylyl cyclase. *Mol Pharmacol* 1996, 50:1–5
24. Zingarelli B, Hasko G, Salzman AL, Szabo C: Effects of a novel guanylyl cyclase inhibitor on the vascular actions of nitric oxide and peroxynitrite in immunostimulated smooth muscle cells and in endotoxic shock. *Crit Care Med* 1999, 27:1701–1707
25. Schmittgen TD, Zakrajsek BA, Mills AG, Gorn V, Singer MJ, Reed MW: Quantitative reverse transcription-polymerase chain reaction to study mRNA decay: comparison of endpoint and real-time methods. *Anal Biochem* 2000, 285:194–204
26. Sammut IA, Foresti R, Clark JE, Exon DJ, Vesely MJ, Sarathchandra P, Green CJ, Motterlini R: Carbon monoxide is a major contributor to the regulation of vascular tone in aortas expressing high levels of haeme oxygenase-1. *Br J Pharmacol* 1998, 125:1437–1444
27. Fujita T, Toda K, Karimova A, Yan SF, Naka Y, Yet SF, Pinsky DJ: Paradoxical rescue from ischemic lung injury by inhaled carbon monoxide driven by derepression of fibrinolysis. *Nat Med* 2001, 7:598–604
28. Chapman HA: Plasminogen activators, integrins, and the coordinated regulation of cell adhesion and migration. *Curr Opin Cell Biol* 1997, 9:714–724
29. Ohashi Y, Kita S, Murakami T: Microcirculation of the rat small intestine as studied by the injection replica scanning electron microscope method. *Arch Histol Jpn* 1976, 39:271–282
30. Choi AM, Alam J: Heme oxygenase-1: function, regulation, and implication of a novel stress-inducible protein in oxidant-induced lung injury. *Am J Respir Cell Mol Biol* 1996, 15:9–19
31. Maines MD: The heme oxygenase system: a regulator of second messenger gases. *Annu Rev Pharmacol Toxicol* 1997, 37:517–554
32. Utz J, Ullrich V: Carbon monoxide relaxes ileal smooth muscle through activation of guanylate cyclase. *Biochem Pharmacol* 1991, 41:1195–1201
33. Brune B, Ullrich V: Inhibition of platelet aggregation by carbon monoxide is mediated by activation of guanylate cyclase. *Mol Pharmacol* 1987, 32:497–504
34. Ramos KS, Lin H, McGrath JJ: Modulation of cyclic guanosine monophosphate levels in cultured aortic smooth muscle cells by carbon monoxide. *Biochem Pharmacol* 1989, 38:1368–1370
35. Otterbein LE, Mantell LL, Choi AM: Carbon monoxide provides protection against hyperoxic lung injury. *Am J Physiol* 1999, 276:L688–L694
36. Otterbein LE, Zuckerbraun BS, Haga M, Liu F, Song R, Usheva A, Stachulak C, Bodyak N, Smith RN, Csizmadia E, Tyagi S, Akamatsu Y, Flavell RJ, Billiar TR, Tzeng E, Bach FH, Choi AM, Soares MP: Carbon monoxide suppresses arteriosclerotic lesions associated with chronic graft rejection and with balloon injury. *Nat Med* 2003, 9:183–190
37. Gunther L, Berberat PO, Haga M, Brouard S, Smith RN, Soares MP, Bach FH, Tobiasch E: Carbon monoxide protects pancreatic beta-cells from apoptosis and improves islet function/survival after transplantation. *Diabetes* 2002, 51:994–999
38. Zhang X, Shan P, Otterbein LE, Alam J, Flavell RA, Davis RJ, Choi AM, Lee PJ: Carbon monoxide inhibition of apoptosis during ischemia-reperfusion lung injury is dependent on the p38 mitogen-activated protein kinase pathway and involves caspase 3. *J Biol Chem* 2003, 278:1248–1258
39. Petrache I, Otterbein LE, Alam J, Wiegand GW, Choi AM: Heme oxygenase-1 inhibits TNF-alpha-induced apoptosis in cultured fibroblasts. *Am J Physiol* 2000, 278:L312–L319
40. Shah KA, Shurey S, Green CJ: Apoptosis after intestinal ischemia-reperfusion injury: a morphological study. *Transplantation* 1997, 64:1393–1397
41. Bolli R, Shinmura K, Tang XL, Kodani E, Xuan YT, Guo Y, Dawn B: Discovery of a new function of cyclooxygenase (COX)-2: COX-2 is a cardioprotective protein that alleviates ischemia/reperfusion injury and mediates the late phase of preconditioning. *Cardiovasc Res* 2002, 55:506–519
42. Foresti R, Motterlini R: The heme oxygenase pathway and its interaction with nitric oxide in the control of cellular homeostasis. *Free Radic Res* 1999, 31:459–475